Proceedings of the ASME 2015 34th International Conference on Ocean, Offshore and Arctic Engineering
OMAE2015
May 31-June 5, 2015, St. John's, Newfoundland, Canada

OMAE2015-41400

NONLINEAR INTERACTIONS IN CROSSING SEA STATES

Joseph Brennan
School of Mathematical Sciences
University College Dublin
Ireland

Frédéric Dias *
School of Mathematical Sciences
University College Dublin
Ireland

ABSTRACT

Presented here is a study on the nonlinear effects contributing to extreme events in wave fields characterised by the presence of two distinct spectral peaks, otherwise known as crossing sea states. Simulations based within the framework of the nonlinear Schrödinger equation have shown that the coupling of two wave groups impinging at various angles strongly influences the growth rate of the Benjamin Feir instability, with various angles enhancing the instability and the characteristics of the rogue event itself. This investigation is based on the more general framework of the Euler equations, employing a Higher Order Spectral Method (HOSM) to numerically solve these equations and obtain the time evolution of the crossing sea state.

INTRODUCTION

Research on oceanic rogue waves has seen increasingly strong interest over the past decade, providing physical understanding of the generation mechanisms and occurrence of such extremes on the open ocean. Kharif *et al.* [1], Dysthe *et al.* [2], and Adcock *et al.* [3], for example, have published reviews on the topic. In addition, field observations of rogue waves (for example, the well known "Andrea" [4] and "Draupner" [5] waves) provide evidence, data, and indeed fuel for the investigation of this phenomenon. Maritime disasters, such as the Suwa-Maru [6] and the Louis Majesty [7] incidents, have been attributed to the presence of such extreme events.

The Draupner, Suwa-Maru, and Louis Majesty events all have one thing in common; they all appear to have occurred in a crossing sea state. Such a sea state is composed of two distinct wave systems propagating with different directions relative to each other, i.e., the corresponding directional spectrum contains two distinct peaks. Such a condition is not uncommon in the open ocean, and as such the rogue wave dynamics in such sea states has received appropriate attention.

Theoretically, coupled Nonlinear Schrödinger Equations have been used in the study of crossing wave-trains and their nonlinear interactions, and in particular, the Benjamin Feir Instability. Narrowband wave trains are well known to be susceptible to this effect (i.e., unstable to sideband perturbations), and the instability has been studied thoroughly in terms of the nonlinear Schrödinger Equation (NLS) for deep water narrowband wave envelopes. Indeed, the Benjamin Feir instability has been put forward as a possible generating mechanism for rogue waves, given the appropriate conditions. Onorato *et al.* [8] derived a set of coupled NLS equations (cNLS) in 2 + 1 dimensions to study the instability in non-collinearly propagating wave trains, and performed stability analysis for perturbations confined to the x axis (i.e. propagation in one dimension). Shukla *et al.* [9], using these equations, performed similar analysis for propagation in two dimensions.

Performing a stability analysis on the cNLS, both papers derive an expression for the growth rate of modulational instabilities in the crossing wave trains, both of which coincide for the case of propagation in one dimension. The analysis indicates that the growth rate of instabilities in such a system is in fact dependent on the angle between the directions of propagation of each wave train. For propagation directions (k,l) and $(k,-l)$, and the angle between is $\alpha = 2\tan^{-1}(l/k)$. The growth rate becomes

*Also at CMLA, ENS Cachan, France

negative at critical angle $\alpha_c = 2\tan^{-1}(1/\sqrt{2}) = 70.53°$, and so focusing instability was found for angles $0 < \alpha < 70.53°$. The instabilities become defocusing after this point, and nonlinear interactions were found to strengthen as crossing angle approached α_c.

Onorato *et al.* [10] and Tofolli *et al.* [11] have taken this further by performing simulations based on the free surface Euler equations, from which the NLS is derived using assumptions of narrow bandwidth and weak nonlinearity. The evolution equations for the free surface are numerically solved via a Higher Order Spectral Method (HOSM), and initialised via a Joint North Sea Wave Observation Project (JONSWAP) spectrum, in deep water. In their work, the time evolution of a sea state comprised of two identical JONSWAP spectra with peak period $T_p = 1s$ was computed for various crossing angles. To examine the potential rogue wave activity in the crossing sea states, kurtosis is measured as a function of crossing angle. Kurtosis itself has a well understood relation to the occurrence of rogue waves, and it is reported in both papers that larger values of kurtosis are found as crossing angle increases towards the α_c, with maximum kurtosis appearing for crossing angles $40° < \alpha < 60°$. These results fall in line with the cNLS stability analysis, and display the increasing importance of nonlinear interactions as crossing angle increases.

Within the present work, we discuss the presence of nonlinear interactions characterised by Benjamin Feir type instabilities in directional crossing sea states, via analysis of HOSM type simulations initialised with directional JONSWAP spectra. However, the spectra considered here within differ from previous efforts in this area in the fact that they contain moderate directional spreading and are defined by wave characteristics which are typical of those found in the open ocean. Also, we conclude that the Benjamin Feir instability is not such an important generating mechanism for rogue waves in such directional states.

MATHEMATICAL FORMULATION

Higher Order Spectral Method

The irrotational flow of an inviscid and incompressible fluid may be adequately described by the velocity potential $\phi(x,y,z,t)$, which within the domain of the fluid, satisfies the Laplace equation. Additionally, the velocity potential also satisfies a kinematic and dynamic boundary condition on the free surface $\eta(x,y,t)$, and so the dynamics of fluid flow may be collectively described by the Euler equations

$$\nabla^2\phi = 0, \qquad \text{for} \quad -\infty < z < \eta(x,y,t) \tag{1}$$

$$\phi_t + gz + \frac{1}{2}(\nabla\phi)^2 = 0, \qquad \text{at} \quad z = \eta(x,y,t) \tag{2}$$

$$\eta_t + \nabla_h\phi\cdot\nabla_h\eta = \phi_z, \qquad \text{at} \quad z = \eta(x,y,t) \tag{3}$$

where ∇_h is the gradient operator in the x-y plane. Defining the velocity potential on the free surface as

$$\psi(x,y,t) = \phi(x,y,z=\eta,t), \tag{4}$$

the free surface boundary conditions (Eqns. (2) - (3)) may be rewritten as

$$\psi_t + g\eta + \frac{1}{2}(\nabla_h\psi)^2 - \frac{1}{2}W^2\left\{1+(\nabla_h\eta)^2\right\} = 0, \tag{5}$$

$$\eta_t + \nabla_h\psi\cdot\nabla_h\eta - W\left\{1+(\nabla_h\eta)^2\right\} = 0, \tag{6}$$

where

$$W = \left.\frac{\partial\phi}{\partial z}\right|_{z=\eta(x,y,t)}, \tag{7}$$

represents the vertical velocity on the free surface.

In order to numerically solve the Euler equations while satisfactorily dealing with the inherent nonlinearity in the boundary conditions, Dommermuth & Yue [16] and West *et al.* [17] independently developed the HOSM in 1987. Each version differs slightly in their method for determining W; West *et al.*'s version has superior consistency between numerical and analytical results, however, and as such their version is the one used here. Tanaka [18] has presented a full description of the method; herein follows a brief description. The Laplace equation for ϕ is directly solved at each time step by assuming a periodic series expansion in the wave steepness ε as solution. A series solution for W is then evaluated, which allows the time evolution of the η and ψ to be followed via Eqns. (5)-(6). The premise of these expansions are to turn a complicated Dirichlet problem on the boundary $z = \eta$ into a series of simpler Dirichlet problems on the boundary $z = 0$, through use of a clever Taylor expansion of the velocity potential on the free surface around $z = 0$.

The series expansions for W and ϕ are is as follows:

$$\begin{aligned} W(x,y,t) &= \sum_{m=0}^{M} W^{(m)}, \\ W^{(m)} &= \sum_{k=0}^{m} \frac{\eta^k}{k!}\frac{\partial^{k+1}}{\partial z^{k+1}}\phi^{(m-k)}(x,y,0,t), \\ \phi^{(1)}(x,y,0,t) &= \psi(x,y,t), \\ \phi^{(m)}(x,y,0,t) &= -\sum_{k=1}^{m}\frac{\eta^k}{k!}\frac{\partial^k}{\partial z^k}\phi^{(m-k)}(x,y,0,t). \end{aligned} \tag{8}$$

$\phi^{(m)}$ and $W^{(m)}$ are assumed to be of order $O(\varepsilon^m)$, and M is the order of nonlinearity. The nonlinear terms present in Eqns. (5)-(6) are smoothly ramped up via the Dommermuth ramping function [19] over ramp time $T_r \approx O(5)T_p$, as in Xiao *et al.* [12]

A third order HOSM expansion has been shown in [18] to be equivalent physically to Zakharov's Hamiltonian formalism, and thus M is chosen as such. Nonlinear interactions between free and bound wave modes are an intrinsic feature to the Euler equations, making the HOSM quite suitable for studying nonlinear rogue wave generation mechanisms, (e.g. Benjamin Feir type instabilities).

CROSSING JONSWAP SPECTRUM

The initial conditions for $\eta(x,y,t)$ and $\phi(x,y,t)$, are constructed using a directional spectrum $E(\omega,\theta)$ consisting of two identical JONSWAP spectral peaks. The spectrum itself is an empirical model describing a growing wave spectrum, based on data collected during the Joint North Sea Wave Project, developed by Hasselmann *et al.* [20]. The spectrum is essentially an extension of the Pierson-Moskowitz spectrum, incorporating a peak shape parameter γ, leading to enhanced nonlinear interactions. In terms of radial frequency ω, it is given by

$$S_j(\omega) = \alpha_p \frac{g^2}{\omega^5} \exp\left[-\frac{5}{4}\left(\frac{\omega_p}{\omega}\right)^4\right] \gamma^{\exp\left[-\frac{1}{2}\left(\frac{\omega-\omega_p}{\sigma\omega_p}\right)^2\right]}, \qquad (9)$$

where the 'p' subscript denotes peak values, α_p is the steepness parameter related to γ, and

$$\sigma = \begin{cases} 0.07, & \omega_p \geq \omega, \\ 0.09, & \omega_p < \omega. \end{cases}$$

Directionality is introduced via a cosine-squared directional function:

$$D(\theta) = \begin{cases} \frac{2}{\Delta\theta}\cos^2\left(\frac{\pi\theta}{\Delta\theta}\right), & |\theta| \leq \Delta\theta/2, \\ 0, & |\theta| > \Delta\theta/2, \end{cases} \qquad (10)$$

where $\Delta\theta$ is the desired directional spreading. The directional spectrum is then given by $E(\omega,\theta) = S_j(\omega)D(\theta)$.

The JONSWAP spectra are computed with spectral peaks at wavenumber $k_p = 0.033m^{-1}$, which in deep water corresponds to a peak period $T_p = 11.087s$, (and $\omega_p = 0.57 rad/s$), which are typical characteristics found in ocean waves. Wave steepness is set at $\varepsilon = 0.16$, which is large enough to trigger potential Benjamin Feir effects, but low enough that wave breaking should not be prominent feature. Moderate directional spreading is considered, so directional bandwidth $\Delta\theta = 21^\circ$ (the intermediate directional spread considered by Xiao *et al.*) and peak enhancement factor $\gamma = 3.3$ are chosen. Two crossing angles within the focusing limit are examined, $\pi/8$ and $\pi/4$ radians, as seen in Figs. 1 & 2. $\alpha = \pi/4$, falls within the area of maximum kurtosis crossing angle region, $40^\circ < \alpha < 60^\circ$, whereas $\alpha = \pi/8$ is on the lower end.

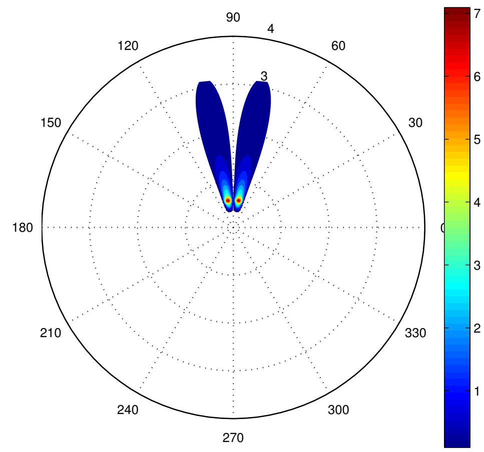

FIGURE 1. Crossing directional spectrum $E(\omega,\theta)$, crossing angle $\alpha = \pi/8$. Circles depict angular frequency (inner ring, 1 rad/s, outer ring, 4 rad/s)

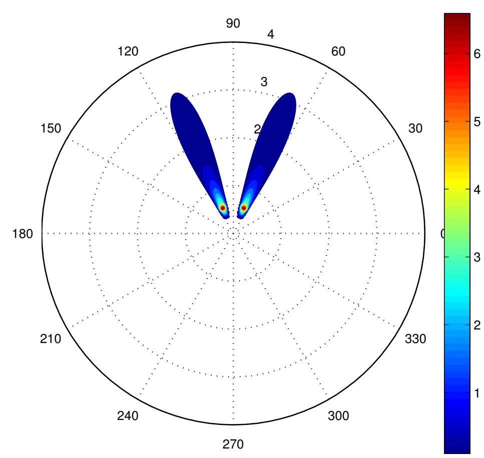

FIGURE 2. Crossing directional spectrum $E(\omega,\theta)$, crossing angle $\alpha = \pi/4$. Circles depict angular frequency (inner ring, 1 rad/s, outer ring, 4 rad/s)

Initial conditions for η and ψ are extracted from $E(\omega,\theta)$ in the following manner. An approximation to random phase is introduced as

$$E(\omega,\theta) \rightarrow E(\omega,\theta)exp(i\beta), \tag{11}$$

where β is normally distributed over $[0,2\pi]$. The spectrum is then converted to the wavenumber domain via the deepwater dispersion relation, and normalised with respect to the conversion. This yields the wavenumber spectrum for η:

$$\hat{\eta}(k_x,k_y) = \frac{1}{2}\frac{g^{1/2}}{|k|^{3/2}}\left(E(k_x,k_y)+c.c.\right), \tag{12}$$

where $c.c.$ denotes the complex conjugate. Linear wave theory yields $\hat{\psi}$ and, finally, the initial condition for η and ψ is obtained via an inverse two dimensional FFT. As such, the HOSM is initialised as a linear wave field, with non-linear terms smoothly ramped up as described earlier.

NUMERICAL SIMULATIONS

Due to the particular interest in Benjaim Feir instability, domains and runtimes are selected with respect to the corresponding physics. As such, timescales are chosen in accordance with the Benjamin Feir timescale ([25], [12]), $T/T_p \sim O(\varepsilon^{-2})$. Similarly, physical domain size is chosen so that $L_{x,y}k_p \sim O(\varepsilon^{-2})$, where wave steepness is $\varepsilon = k_pH_s/2$. A balance between resolution and computational speed is necessary, so $256x256$ Fourier modes are used. Time integration was handled via a Dormand-Prince-Shampine Runge-Kutta scheme, with time step set to $\Delta t = 0.02s$ to minimise energy leakage.

In order to investigate the potential activity of Benjamin-Feir type instabilities, the fourth order moment of surface elevation, kurtosis, is measured. Kurtosis has a well known correlation with the Benjamin Feir index (BFI), a measure of a wave field's susceptibility to the Benjamin Feir Instability. The BFI is the ratio between steepness and bandwidth; $BFI = \varepsilon k_p/\Delta k$, and its relationship with kurtosis is given by $Kur = 3+2\pi BFI^2/\sqrt{3}$ (See Janssen [21] and Mori & Janssen [22]. Directional spreading has a damping effect on kurtosis, and indeed BFI, and as the wave fields being examined are constructed with a moderate directional spread, excess kurtosis (i.e., the divergence from the Gaussian value of 3), is not expected to be large.

Time evolution of skewness and kurtosis are presented in Figs. 3 & 4, computed over ~ 60 HOSM simulations. The impact of even moderate directional spreading is as expected, as in both cases, kurtosis is seen to be weakly non-gaussian, with negative excess kurtosis seen for $\alpha = \pi/8$. Interestingly, for $\alpha = \pi/4$, there is a clear increase in kurtosis, and so despite the directional dampening effects, kurtosis still increases with crossing angle. It can be thus observed that in directional crossing sea states, nonlinear interactions characterised by Benjamin Feir type instabilities become more important in the dynamics of the sea state with increased crossing angle. However, Benjamin Feir instability is not expected to feature prominently in the generation of rogue waves in such sea states.

Skewness does not seem to be influenced significantly by crossing angle, with consistent positive non-gaussian values (~ 0.1) indicating a bias towards large crest heights.

CONCLUSIVE REMARKS

In the present work, we have examined nonlinear effects in directional crossing sea states via Higher Order Spectral Method (HOSM) simulations. Similar studies have been performed by [10] and Tofolli *et al.* [11] for high frequency wave fields. Their work highlighted the influence of crossing angle on Benjamin Feir Instabilities, and angles of particular interest were used here within to study crossing sea states with moderate directional spreading and characteristics resembling those of oceanic waves. Kurtosis, which has a well known relationship with the Benjamin Feir index, are measured in order to identify the potential for such instabilities to occur.

Our results indicate that for directional crossing sea states, such nonlinear effects are indeed enhanced by increased crossing angle. Weakly non-gaussian values of kurtosis imply, however, that the Benjamin Feir instability is not necessarily an important factor in the generation of rogue waves in such sea states. For lower crossing angles, these effects are much weaker.

Further investigation is required to understand the dynamics between crossing sea states and rogue waves. Much of the work here is theoretical, and the crossing spectra analysed are very simplistic compared to those found in the open ocean (for example, see Ponce de León *et al.* [23] . It has been suggested in [6] that freakish sea states can occur as a result of nonlinear interaction between wind-waves and swell, over much larger timescales ($\sim O(10^3)T_p$) than those considered here. At such timescales, wind influence would become an important factor, and so different models (for example, wave spectral models) may need to be considered.

This work is based upon works supported by the European Research Council (ERC) under the research project ERC-2011-AdG 290562-MULTIWAVE and Science Foundation Ireland under grant number SFI/12/ERC/E2227. The authors would also like to acknowledge Claudio Viotti for his contributions to the development of the HOSM code, and the Irish Centre for High-End Computing for access to the Fionn supercomputer system.

REFERENCES

[1] KHARIF, C., & PELINOVSKY, E., 2003. Physical mechanisms of the rogue wave phenomenon. *European Journal of Mechanics B/Fluids*, **22**, 603-634.

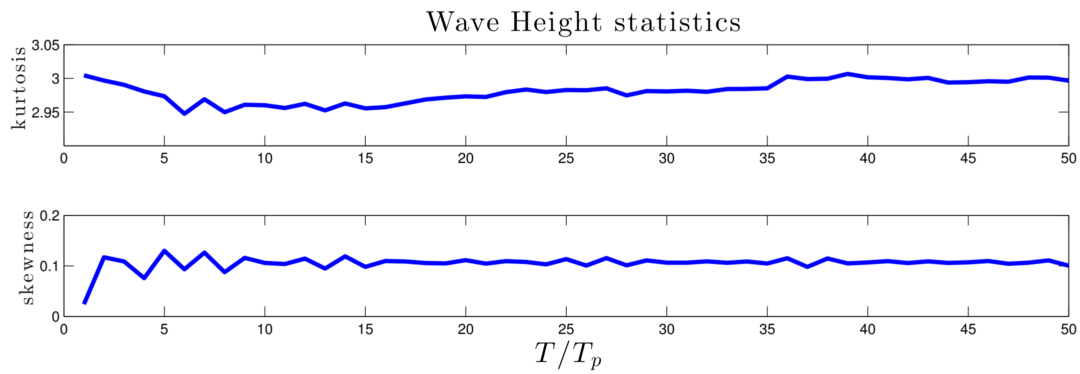

FIGURE 3. Statistical analysis of wave field simulated by HOSM, with crossing angle $\alpha = \pi/8$. Top: Kurtosis, Bottom: Skewness.

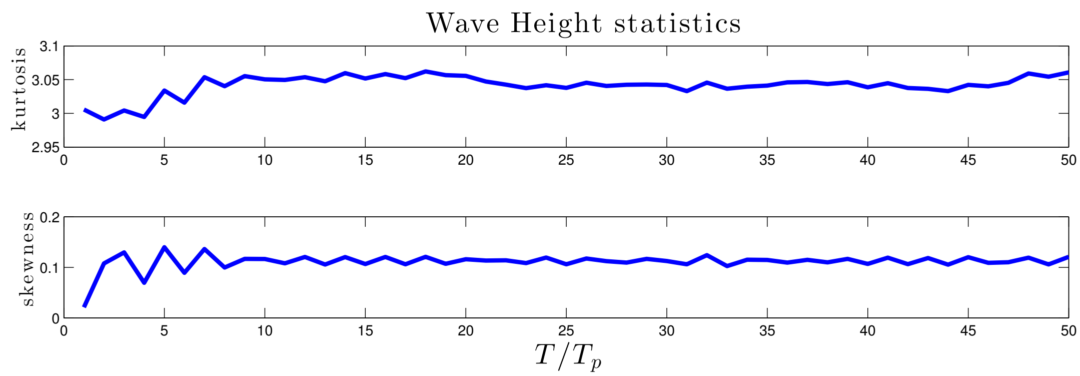

FIGURE 4. Statistical analysis of wave field simulated by HOSM, with crossing angle $\alpha = \pi/4$. Top: Kurtosis, Bottom: Skewness.

[2] DYSTHE, K., KROGSTAD, H.E., & MULLER, P., 2008. Oceanic Rogue Waves. *Annu. Rev. Fluid Mech.*, **40**, 287-310.

[3] ADCOCK, T.A.A., & TAYLOR, P.H., 2014. The Physics of Anomalous ('Rogue') Ocean Waves/ *Rep. Prog. Phys.* **77** (17pp)

[4] MAGNUSSON, A.K., & DONELAN, M.A., 2013. The Andrea Wave Characteristics of a Measured North Sea Rogue Wave. *Journal of Offshore Mechanics and Arctic Engineering*, **135**, 031108-1.

[5] ADCOCK, T., TAYLOR, P.H., YAN, S., MA, Q.W., & JANSSEN, P.A.E., 2011. Did the Draupner Wave occur in a crossing sea? *Proc. R. Soc. A*.

[6] TAMURA, H., WASEDA, T., & MIYAZAWA., Y, 2009. Freakish Sea State and Swell Wind Sea Coupling: Numerical Study of the Suwa Maru Incident. *Geophysical Rev. Lett.*, **36**.

[7] CAVALERI, L., BERTOTTI, L., TORRISI, L., BITNER-GREGERSEN, E., & ONORATO, M., 2012. Rogue Waves in Crossing Seas: The Louis Majesty Accident. *J. Geophysical Research*, **117**.

[8] ONORATO, M., OSBORNE, A.R., & SERIO, M., 2006a. Modulational Instability in Crossing Sea states: A Possible Mechanism for the Formation of Freak Waves. *Phys Rev Lett.*, **96**.

[9] SHUKLA, P.K., KOURAKIS, I., ELIASSON, B., MURKLAND, M., & STENFLO, L., 2006. Instability and Evolution of Nonlinearly Interacting Water Waves. *Phys. Rev. Lett.*, **97**.

[10] ONORATO, M., PROMENT, D., & TOFFOLI, A., 2010. Freak Waves in Crossing Seas. *Eur. Phys. J. Spec. Top*, **185**, 45-55.

[11] TOFFOLI, A., BITNER-GREGERSEN, E.M., OSBORNE, A.R., SERIO, M., & MONBALIU, J, 2011. Extreme Waves in Random Crossing Seas: Laboratory Experiments and Numerical Simulations. *Geophysical Research Letters*, **38**.

[12] XIAO, W., LIU, Y., WU, G., & YUE, D.K.P., 2013. Rogue WAve occurrence and dynamics by direct simulations of nonlinear wave-field evolution. *J. Fluid. Mech*, **720**, 3357–392.

[13] CLAUSS, G.F., KLEIN, M., DUDEK, M., ONORATO, M., 2014. Application of Higher Order Spectral Method for Deterministic Wave Forecast *Proc. ASME 2014* 33^{rd} *International Conference OMAE*, **OMAE2014-24126**, San Francisco, California.

[14] TOFFOLI, A., BABANIN, A., ONORATO, M., & WASEDA,

T., 2010 Maximum Steepness of Oceanic Waves: Field and Laboratory Experiments. *Geophysical Research Letters*, **37**.

[15] GEMMRICH, J., 2005. On the occurrence of wave breaking. *14th 'Aha Huliko'a Hawaiian Winter Workshop on Rogue Waves, January 2005,* 123-130

[16] DOMMERMUTH, D.G., YUE, D.K.P., 1987. A High-Order Spectral Method for the Spectral Method for the Study of Nonlinear Gravity Waves *J. Fluid. Mech.*, **184**, 267-288

[17] WEST, B.J., BRUECKNER, K., & JANDA, R. S., 1987. A New Numerical Method for Surface Hydrodynamics *Journal of Geophysical Research*, **92**, 11,803-11,824

[18] TANAKA, M., 2001. A method of studying nonlinear random field of surface gravity waves by direct numerical simulation. *Fluid Dynamics Research*, **28** 41–60

[19] DOMMERMUTH, D., 2000. The Initialization of Nonlinear Waves Using an Adjustment Scheme. *Wave Motion* ,**32**, 307-317.

[20] HASSELMANN K., BARNETT, T.P., BOUWS, E., CARLSON, H., CARTWRIGHT, D.E., ENKE, K., EWING, J.A., GIENAPP, D.E., HASSELMANN, P., KRUSEMAN, P., MEERBURG, A., MLLER, P., OLBERS, D.J., RICHTER, K., SELL, W., & WALDEN, H., 1973. Measurements of wind-wave growth and swell decay during the Joint North Sea Wave Project (JONSWAP) *Ergnzungsheft zur Deutschen Hydrographischen Zeitschrift Reihe,* **A(8) (Nr. 12)**, p. 95.

[21] JANSSEN, P.A.E.M, 2003. Nonlinear Four-Wave Interactions and Freak Waves. *J. of Phys. Oceanography*, **33**, 863-884

[22] MORI, N., & JANSSEN, P.A.E.M., 2006. On Kurtosis and Occurrence Probability of Freak Waves. *Journal of Physical Oceanography*, **36**, 1471-1483.

[23] PONCE DE LEÓN, S., &GUEDES SOARES, C., 2012 Distribution of Winter Wave Spectral Peaks in the Seas around Norway. *Ocean Engineering* **50** 63-71.

[24] DYSTHE, K., TRULSEN, K., KROGSTAD, E., & SOCQUET-JUGLARD, H., 2003. Evolution of a narrow-band spectrum of random surface gravity waves. *J. Fluid. Mech.*, **478**.

[25] ALBER, I.E., 1978. The Effects of Randomness on the Stability of Two-Dimensional Surface Wavetrains. *Proc. R. Soc. A*, **363**, 525-546.